The Astrophysical Journal, 584:1071–1083, 2003 February 20

OPTICALLY THICK GYROSYNCHROTRON EMISSION FROM ANISOTROPIC ELECTRON DISTRIBUTIONS

G. D. Fleishman[1,2,3] and V. F. Melnikov[4]
Received 2002 July 6; accepted 2002 October 31

ABSTRACT

We present a numerical study of optically thick gyrosynchrotron emission produced by fast electrons with anisotropic pitch-angle distributions. The anisotropy is found to affect substantially both radiation spectra and polarization. The harmonic nature of gyrosynchrotron emission becomes more pronounced for the anisotropic case. The effect is entirely provided by a reduction of the self-absorption coefficient due to pitch-angle anisotropy; thus, it is essentially different from electron cyclotron maser emission, which is due to wave amplification under negative absorption. The paper studies the dependences of the emission on the involved parameters and discusses possible applications of the results to observations of microwave solar radio bursts.

Subject headings: acceleration of particles — Sun: flares — Sun: particle emission — Sun: radio radiation

1. INTRODUCTION

The gyrosynchrotron emission mechanism has been widely used for many astrophysical and solar applications since synchrotron radiation was proposed to interpret nonthermal cosmic radio emission half a century ago (Alfvén & Herlofson 1950; Kiepenheuer 1950; Ginzburg 1951; Getmantsev 1952; Razin 1960; Ginzburg & Syrovatsky 1964; Ramaty 1969; Takakura 1972). For the optically thin regime, most of the papers focused on isotropic distributions of fast electrons. Only a few exceptions consider anisotropic pitch-angle distributions (Petrosian 1982; Robinson 1985; Klein 1987).

For the optically thick regime, a huge number of studies have been done with different anisotropic pitch-angle distributions (e.g., Wu & Lee 1979; Melrose, Rönnmark, & Hewitt 1982; Sharma & Vlahos 1984; Li 1986; Huang 1987; Aschwanden & Benz 1988; Fleishman & Yastrebov 1994; Ledenev 1998; Vlasov, Kuznetsov, & Altyntsev 2002; Fleishman & Melnikov 1998 and references therein), but all of them focused on the conditions required to provide " negative " absorption. The negative absorption by an unstable electron distribution leads to an amplification of gyrosynchrotron radiation, which is currently referred to as electron cyclotron maser (ECM) emission. The mechanism is assumed to be responsible for some types of coherent solar (Fleishman & Melnikov 1998) and stellar (Bastian et al. 1990) emission.

However, the intermediate case, in which the pitch-angle distribution is anisotropic but still does not lead to the ECM emission, has not yet been studied.

Nevertheless, there is ample evidence that the fast electrons are distributed anisotropically in flares. This follows, e.g., from many observations of electron beams propagating along the magnetic field lines in the solar corona (Aschwanden et al. 1990). On the other hand, there are indications of the transverse anisotropy of nonthermal electrons. First of all, there is the prominent directivity of gamma-ray flares (McTiernan & Petrosian 1991) produced by relativistic electrons. Analysis of the effects of particle kinetics on the temporal and spectral behavior of optically thin microwave and hard X-ray emissions (Melnikov 1994; Melnikov & Magun 1998) indicates that a considerable fraction of accelerated particles will accumulate in the loop. While the cited papers do not directly consider any pitch-angle anisotropy, the trapping itself assumes that electrons are lacking within a loss cone (because only electrons with large enough pitch angles can experience magnetic mirroring, while others are lost as a result of precipitation) and, therefore, they are distributed anisotropically. Furthermore, Lee & Gary (2000) found the anisotropic pitch-angle distribution (including anisotropic injection) to be required for explaining an observation of spectral evolution of a microwave burst. Evidence for anisotropic pitch-angle distribution in the transverse direction has been gathered from observation of a bright loop-top source of microwave emission (Melnikov et al. 2001; Kundu et al. 2001), which has been interpreted as tracer of a strong concentration of mildly relativistic electrons trapped and accumulated in the top of a flaring loop (Melnikov, Shibasaki, & Reznikova 2002). A very common process leading to concentration of fast electrons within a loop-top would be the trapping of electrons with large pitch angles as a result of magnetic mirroring. In addition, some acceleration processes result in anisotropic particle distributions (e.g., Pryadko & Petrosian 1999). Thus, nonisotropic pitch-angle distributions of fast electrons are likely to exist.

It is well known (see Fleishman & Melnikov 1998 for a review) that anisotropic pitch-angle distributions could be unstable to produce coherent (ECM or plasma) emissions. The typical timescale of these coherent emissions (provided by wave-particle or/and wave-wave interactions) is of the order of tens of milliseconds under flaring conditions (Fleishman & Arzner 2000), which is much less than typical time of variability of incoherent gyrosynchrotron emission (Bastian, Benz, & Gary1998). Hence, these two types of emission could be clearly distinguished in terms of duration. We should note that even in case an instability develops, the back-reaction of the amplified waves on the initial pitch-angle anisotropy does not necessarily lead to complete

[1] Purple Mountain Observatory, National Astronomical Observatories, Nanjing 210008, People's Republic of China.
[2] Ioffe Institute for Physics and Technology, St. Petersburg 194021, Russia.
[3] New Jersey Institute of Technology, Newark, NJ 07102.
[4] Radiophysical Research Institute (NIRFI), Nizhny Novgorod 603950, Russia.

isotropization (Fleishman & Arzner 2000), while it may modify the anisotropic distribution to some extent to quench the instability.

This paper presents a detailed study of gyrosynchrotron radiation produced by anisotropic electron distributions in the optically thick regime, the completely unexplored corner of the subject. The analysis of the optically thick part of the spectrum allows us to discuss the low-frequency radiation only; the whole spectrum is studied in a companion paper (Fleishman & Melnikov 2003). For simplicity we assume a time-independent particle distribution and magnetic field, since our goal is mainly to investigate the effect of the pitch-angle anisotropy on gyrosynchrotron intensity and polarization spectra.

Direct application of the results obtained in the paper to radio emission from solar flares is obviously limited to observations with instruments having high spatial resolution (resolving regions with relatively constant parameters). Among them are currently operating arrays such as the Nobeyama Radioheliograph (NoRH; Nakajima et al. 1994), the Owens Valley Solar Array (OVSA; Gary & Hurford 1999), the Siberian Solar Radio Telescope (SSRT; Smolkov, Zandanov, & Altyntsev 2000), and the Very Large Array (VLA). Furthermore, the planned Frequency Agile Solar Radiotelescope (FASR; Bastian et al. 1998) will produce high-quality data suitable for such investigation, since it will provide sufficiently high spatial and spectral resolutions along with a wide spectral coverage.

The organization of the paper is as follows. Section 2 describes briefly the general formalism and our calculations. Section 3 presents the results of the calculations through a broad range of the involved parameters. Section 4 discusses the discovered effects, their observability, and their impact on current models of the flaring microwave emission.

2. GENERAL FORMULATION

The gyrosynchrotron emissivity and self-absorption coefficient are calculated by direct integration over momentum space of the emission intensity produced by a single electron in magnetized plasma (Eidman 1958, 1959) with the particle distribution function or their derivatives in the momentum space.

While the particle energy E (or the Lorentz factor γ_e) is usually used as the integration variable (e.g., Ramaty 1969), we chose the momentum p because the momentum (rather than energy E) is the independent variable in the Boltzmann kinetic equation (specifying the distribution function). The transformation from one form to the other is easy to perform with the use of the relativistic relation

$$E^2 = m^2c^4 + p^2c^2 \ , \tag{1}$$

where m is the electron mass and c is the speed of light.

In this study we use the following (factorized) general form of the distribution function:

$$f(\boldsymbol{p}) = \frac{N_e}{2\pi} f_1(p) f_2(\mu) \ , \tag{2}$$

where the (invariant) distribution function $f(\boldsymbol{p})$ is normalized by the number density of fast electrons:

$$\int f(\boldsymbol{p}) p^2 dp\, d\mu\, d\varphi = N_e \ , \tag{3}$$

where μ is the cosine of the particle pitch angle θ, φ is the azimuth angle, and N_e is the number density of fast electrons. The functions f_1 and f_2 are both normalized to unity:

$$\int f_1(p) p^2 dp = 1 \ , \qquad \int_{-1}^{1} f_2(\mu) d\mu = 1 \ . \tag{4}$$

Respectively, the emissivity and self-absorption coefficient receive the form

$$\begin{aligned} j_\sigma(\omega, \vartheta) = & \frac{4\pi^2 e^2}{c} \frac{\omega^2 [\partial(\omega n_\sigma)/\partial\omega]}{(1 + K_\sigma^2 + \Gamma_\sigma^2)} \\ & \times \sum_{n=1}^{\infty} \int \gamma_e \beta^2 d^3p (1 - \mu^2) f(\boldsymbol{p}) \\ & \times \left[\frac{\Gamma_\sigma \sqrt{1 - \eta^2} + K_\sigma(\eta - \beta\mu n_\sigma)}{n_\sigma \beta \sqrt{(1 - \mu^2)(1 - \eta^2)}} J_n(z) + J_n'(z) \right]^2 \\ & \times \delta(\gamma_e \omega - n\omega_{Be} - \gamma_e \beta n_\sigma \eta \mu \omega) \ , \end{aligned} \tag{5}$$

$$\begin{aligned} æ(\omega, \vartheta) = & -\frac{\pi \omega_{pe}^2}{(1 + K_\sigma^2 + \Gamma_\sigma^2)\{2n_\sigma[\partial(\omega n_\sigma)/\partial\omega]\} v_\sigma N} \\ & \times \sum_{n=1}^{\infty} \int d^3p (1 - \mu^2) \\ & \times \left[\frac{\Gamma_\sigma \sqrt{1 - \eta^2} + K_\sigma(\eta - \beta\mu n_\sigma)}{n_\sigma \beta \sqrt{(1 - \mu^2)(1 - \eta^2)}} J_n(z) + J_n'(z) \right]^2 \\ & \times \left[p\frac{\partial}{\partial p} - (\mu - n_\sigma \beta \eta) \frac{\partial}{\partial \mu} \right] f(\boldsymbol{p}) \\ & \times \delta(\gamma_e \omega - n\omega_{Be} - \gamma_e \beta n_\sigma \eta \mu \omega) \ , \end{aligned} \tag{6}$$

where ω_{pe} and $\omega_{\rm Be}$ are the electron plasma- and gyrofrequencies, N is the number density of the background plasma, $\eta = \cos\vartheta$, ϑ is the view angle, $J_n(z)$ and $J_n'(z)$ are the Bessel function and its derivative over argument z, $z = (\omega/\omega_{\rm Be}) \gamma_e n_\sigma \beta \sqrt{(1 - \mu^2)(1 - \eta^2)}$, $\beta = v/c$ is the dimensionless particle velocity, v_σ is the group velocity of the σ-mode wave, and n is the index of summation. Expressions for the refractive indices n_σ and the polarization coefficients K_σ and Γ_σ can be found elsewhere (e.g., Ramaty 1969); we use here the notations accepted in Fleishman (1994; see also the Appendix).

The radiation intensity of each mode from a homogeneous source is obviously given by

$$J_\sigma(\omega, \vartheta) = \frac{j_\sigma(\omega, \vartheta)}{æ_\sigma(\omega, \vartheta)} (1 - e^{-\tau_\sigma}) \ , \tag{7}$$

where $\tau_\sigma = æ_\sigma L$ is the optical depth of the source and L is the source size along the line of sight.

As has been pointed out in the § 1, we restrict our analysis to the optically thick region, $\tau \gg 1$. We thus calculate the ratio

$$J_\sigma(\omega, \vartheta) = \frac{j_\sigma(\omega, \vartheta)}{æ_\sigma(\omega, \vartheta)} \tag{8}$$

for both ordinary (O; $\sigma = 1$) and extraordinary (X; $\sigma = -1$) waves together with the degree of polarization (in the limit of strong Faraday rotation)

$$P(\omega, \vartheta) = \frac{J_X(\omega, \vartheta) - J_O(\omega, \vartheta)}{J_X(\omega, \vartheta) + J_O(\omega, \vartheta)} \ . \tag{9}$$

Accordingly, negative (positive) polarization corresponds to predominant O- (X-) mode radiation.

To calculate $j_\sigma(\omega, \vartheta)$ and $æ_\sigma(\omega, \vartheta)$, we used numerical Gaussian integration routine. The derivatives of the distribution function were taken analytically, and Bessel functions were calculated by exact expressions, while their derivatives were calculated with the use of recurrent relations. The integrals were taken with the accuracy 10^{-3}. The results obtained for isotropic pitch-angle distribution were checked against those obtained with Ramaty's code (Ramaty et al. 1994).

3. NUMERICAL RESULTS

We chose a power-law distribution of the electrons over momentum:

$$f_1(p) = \frac{(\gamma - 3)p_0^{\gamma-3}}{p^\gamma} , \qquad p_{\min} < p < p_{\max} , \qquad (10)$$

with $p_{\min} = 0.2mc$ ($E_{\rm kin} \approx 10$ keV) and $p_{\max} = 20mc$ ($E \approx 10$ MeV), which was checked to be sufficient for the low-frequency (optically thick) range by varying $p_{\max}$. Most of the calculations was performed for a loss-cone

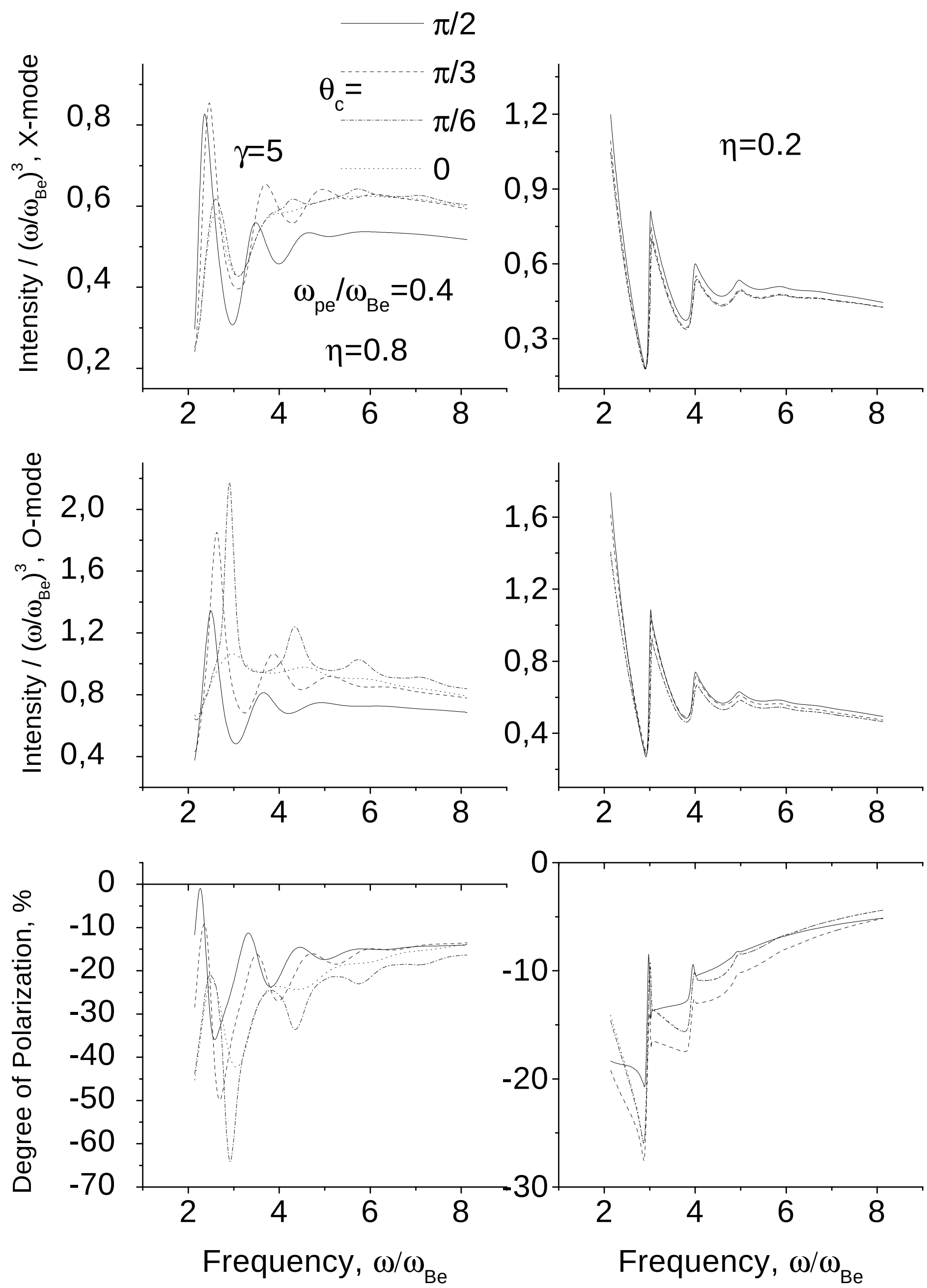

FIG. 1.—Gyrosynchrotron radiation intensity and degree of polarization vs. frequency for various θ_c in sin-N pitch-angle distribution. The parameters are shown in the figure. The differences in intensity and polarization for different loss-cone angles θ_c are most pronounced for quasi-parallel to the magnetic field wave emission ($\eta = 0.8$).

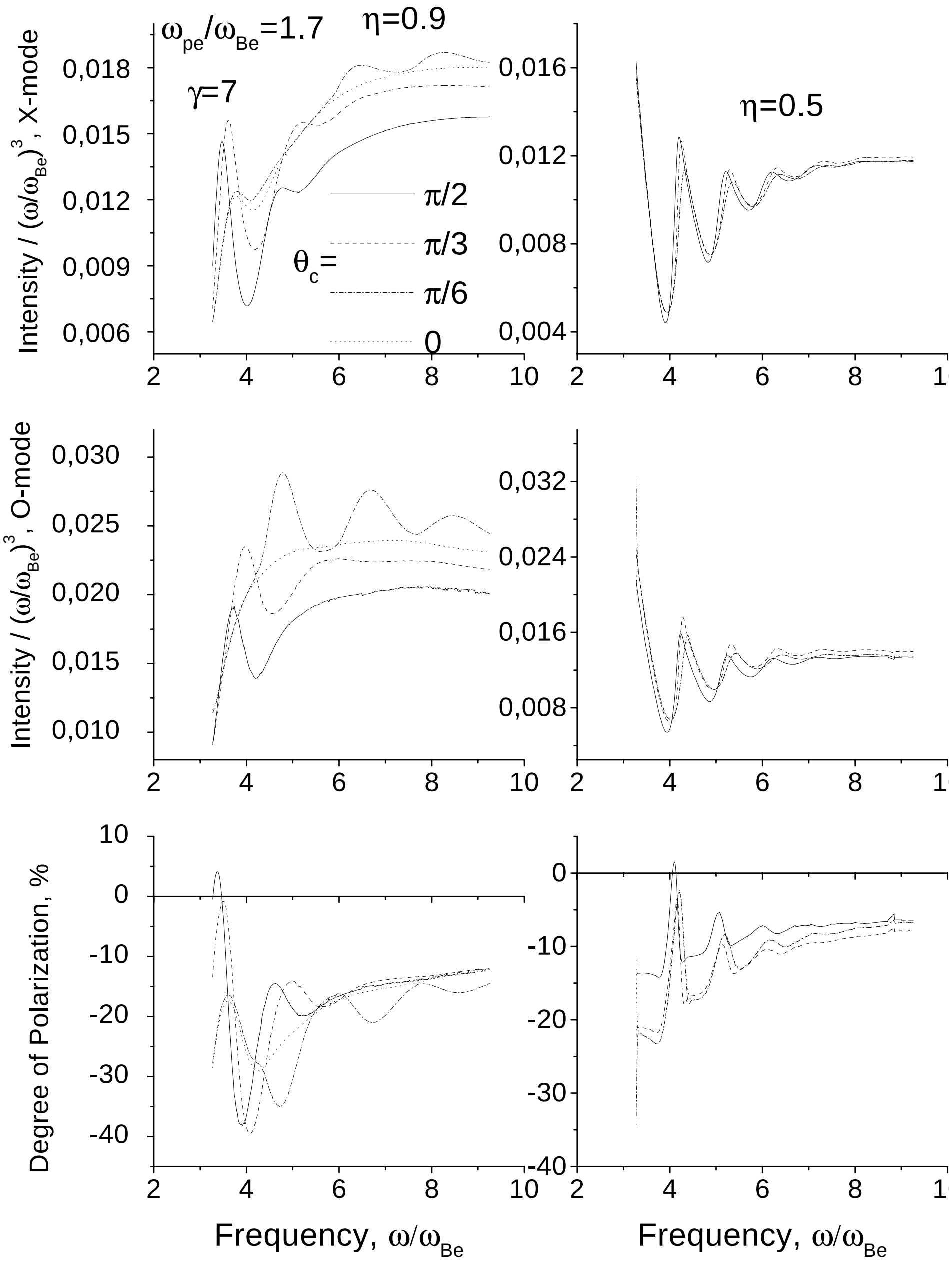

FIG. 2.—Same as in Fig. 1, but for higher plasma- to gyrofrequency ratio ($\omega_{pe}/\omega_{\rm Be} = 1.7$) and spectral index $\gamma = 7$. The anisotropy makes spectral structure in intensity and polarization more pronounced.

pitch-angle distribution modeled by a function that varies as a power of a sine function of the pitch angle (hereafter "sin-N function"; Hewitt, Melrose, & Rönnmark 1982):

$$f_2(\mu) \propto \begin{cases} \text{sin-N}\left(\dfrac{\pi}{2}\dfrac{\theta}{\theta_c}\right) , & 0 < \theta < \theta_c , \\ 1 , & \theta_c < \theta < \pi - \theta_c , \\ \text{sin-N}\left[\dfrac{\pi(\theta - \pi)}{2\theta_c}\right] , & \pi - \theta_c < \theta < \pi , \end{cases} \tag{11}$$

while a few runs were performed for a Gaussian angular distribution:

$$f_2(\mu) \propto \exp(-(\mu - \mu_1)^2/\mu_0^2) . \tag{12}$$

The radiation intensity (and polarization) depends on a few involved parameters: plasma parameter $Y = \omega_{pe}/\omega_{\rm Be}$, loss-cone angle θ_c, loss-cone steepness N, spectral index γ, view angle ϑ, and frequency ω of emission.

We varied all these parameters in our calculations. The main set of plots represents the dependences of the X and O radiation intensities and the degree of polarization on frequency for $N = 6$ and various values of Y, γ, and θ_c. We plotted the intensity divided by dimensionless factor $(\omega/\omega_{\rm Be})^3$ rather than intensity itself to make all spectral features (peaks) more visible, because the mean value of the intensity varies approximately as ω^3 in the optically thick region (Dulk & Marsh 1982). Even a brief look at the figures reveals a significant effect of the pitch-angle anisotropy on the radiation. Let us describe the results in more detail.

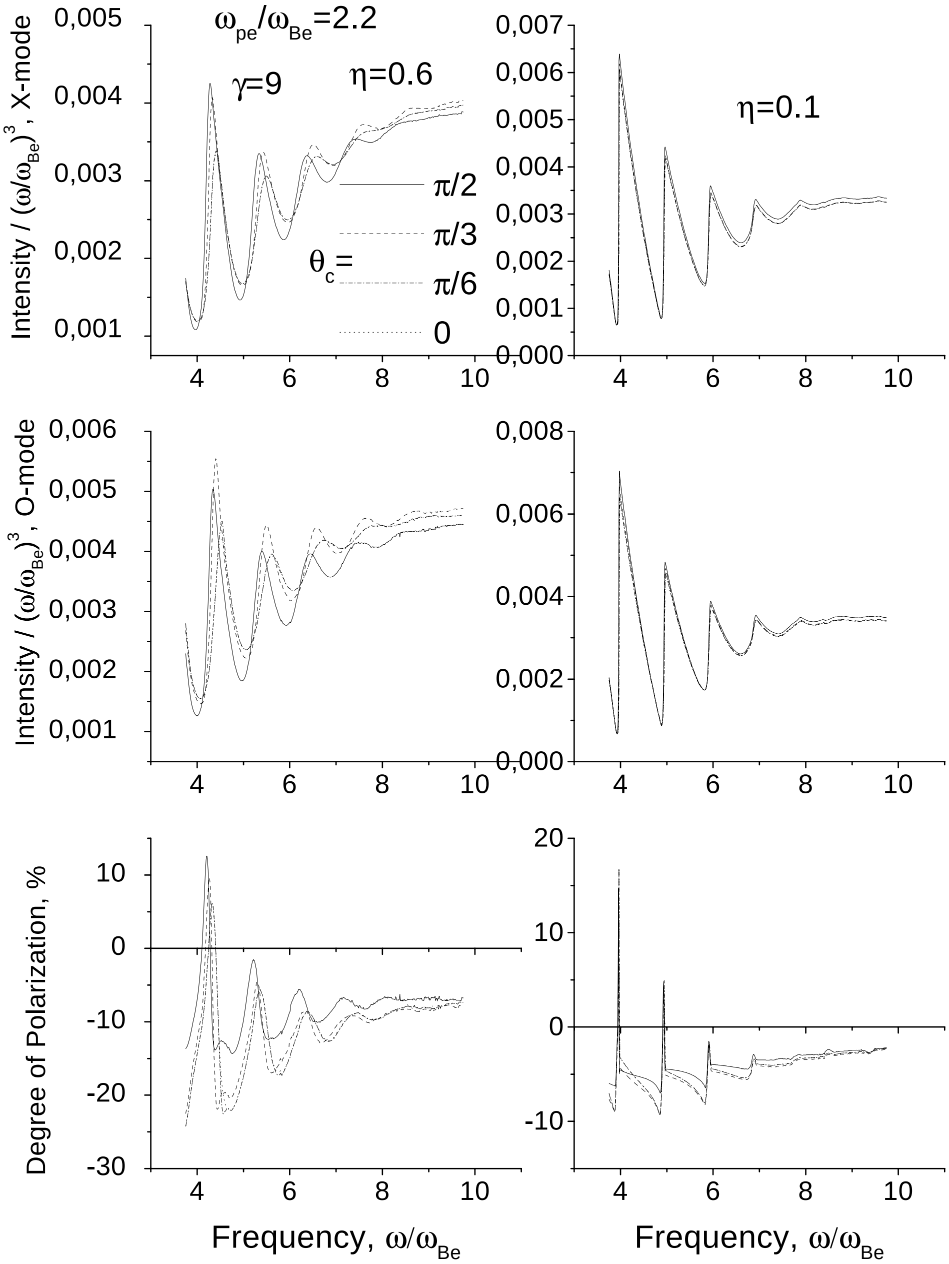

FIG. 3.—Same as in Fig. 1, but for $\omega_{pe}/\omega_{\rm Be} = 2.2$ and spectral index $\gamma = 9$

Spectral peaks.—Low-frequency gyrosynchrotron emission is known (e.g., Benka & Holman 1992; Zhou & Huang 2001) to display spectral peaks due to contribution of a few of the lowest harmonics of the gyrofrequency. Figures 1–3 demonstrate that the peaks become more pronounced and numerous for the anisotropic pitch-angle distribution.

Figure 1 displays the case of relatively tenuous plasma ($Y = 0.4$) and hard spectrum of fast electrons ($\gamma = 5$). The anisotropic distribution provides more peaks (and the peaks become more prominent) than the isotropic distribution for quasi-parallel to the magnetic field wave emission ($\eta = 0.8$) for both X and O waves (Fig. 1, *left column*). Respectively, the degree of polarization (Fig. 1, *left bottom*) reveals stronger variations as frequency changes than in the isotropic case.

It is remarkable that the frequencies of the spectral peaks are not fixed to the integer multiples of the gyrofrequency but vary depending on the loss-cone angle θ_c. For instance, Figure 1 shows that the emission with $\theta_c = \pi/6$ has a local maximum at $\omega/\omega_{\rm Be} \approx 4.4$, but the emission with $\theta_c = \pi/3$ has a local minimum at the same frequency. This is an extreme example of a more general tendency of nonmonotonic change in the intensity with the loss-cone angle θ_c.

The anisotropy of the "loss-cone" type has weaker effect on the emission in the quasi-transverse directions ($\eta = 0.2$; Fig. 1, *right column*): the number of peaks and their bandwidth are similar to those in the isotropic case. Nevertheless, the degree of polarization can change noticeably (Fig. 1, *right bottom*).

Typically, the described spectral structure becomes less pronounced for larger plasma frequency to gyrofrequency ratios (Fig. 2, $Y = 1.7$) because of the effect of density (for synchrotron radiation produced by ultrarelativistic

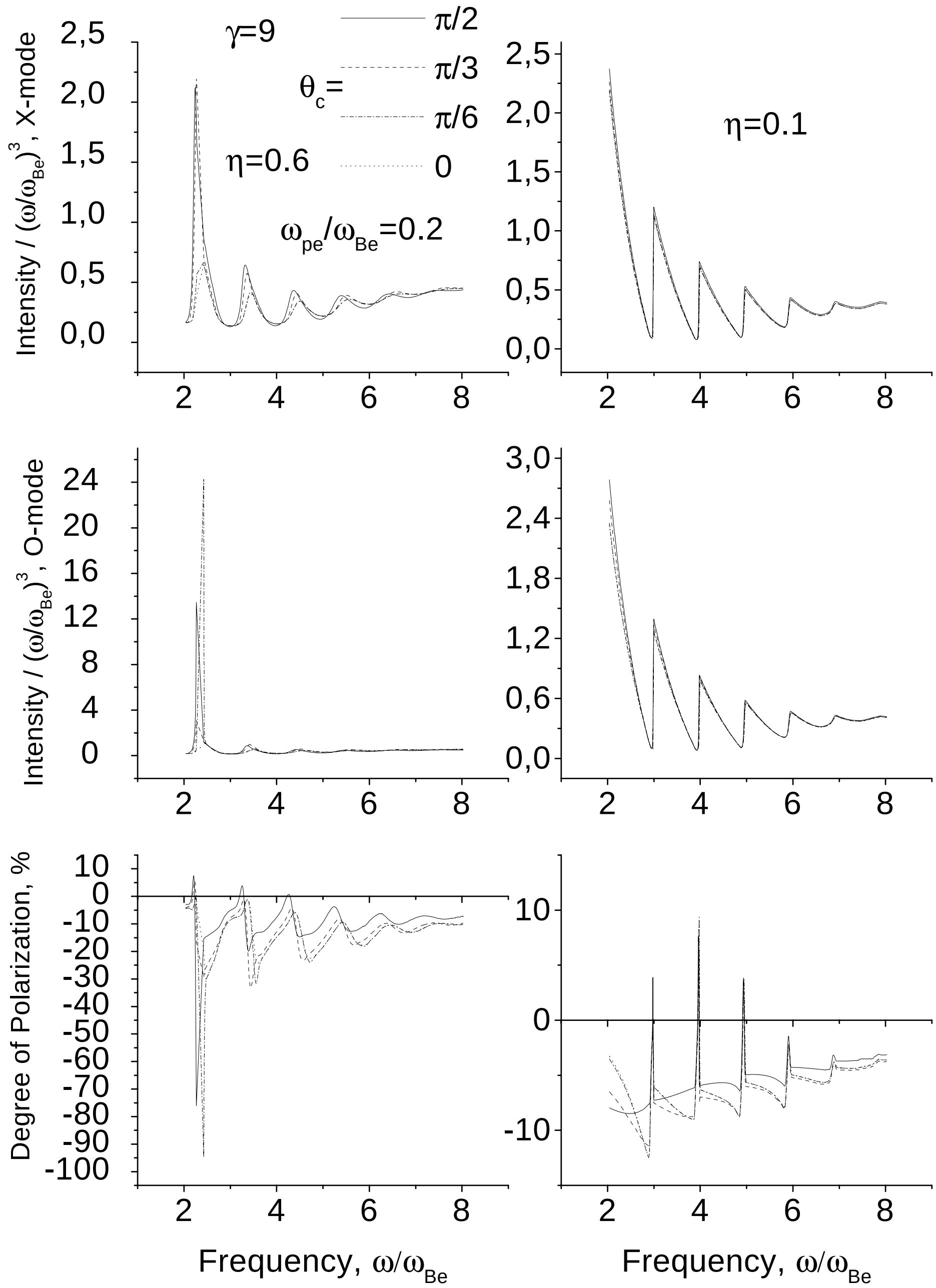

FIG. 4.—Example of a strong narrow peak. The emission of *O*-mode displays a strong narrow peak at $\omega/\omega_{Be} = 2.2$–2.3 with the degree of polarization close to 100% for the quasi-parallel direction (*middle left*). Quasi-transverse radiation is weakly sensitive to the anisotropy when the other parameters remain the same.

electrons, the effect of density is referred usually to as the Razin effect, which gives rise to exponential fall of the emission at low frequencies [Razin 1960]). Indeed, no harmonic structure is visible for the isotropic case in Figure 2 ($\eta = 0.9$; *left column*). Nevertheless, anisotropic distribution can produce spectral peaks up to $\omega/\omega_{\rm Be} \sim 10$. The number of visible spectral peaks changes with θ_c nonmonotonically. For example, *O*-mode intensity (Fig. 2, *middle left*) displays three peaks for $\theta_c = \pi/3$ but only one for both $\theta_c = \pi/2$ and $\theta_c = \pi/6$. The degree of polarization displays spectral variations as well. For quasi-transverse emission ($\eta = 0.5$; Fig. 2, *right column*) the harmonic structure is evident for both the isotropic and anisotropic cases. The anisotropy has a weak effect on radiation intensity of both the *X*- and *O*-mode waves, while it has a noticeable effect on the degree of polarization.

Figure 3 displays emission produced by softer electron spectrum ($\gamma = 9$) in denser plasma ($Y = 2.2$). The softer spectrum produces more spectral peaks (even for isotropic case) than hard electron distributions in Figures 1 and 2, because the contribution of low-energy electrons is more important here. The emission by low-energy electrons displays more clear harmonic structure because the Doppler effect provides weaker spectral smoothing in this case. The effect of anisotropy becomes weaker as Y increases or η decreases.

It is well known (see Fleishman & Melnikov 1998 for a review) that anisotropic electron distributions can produce

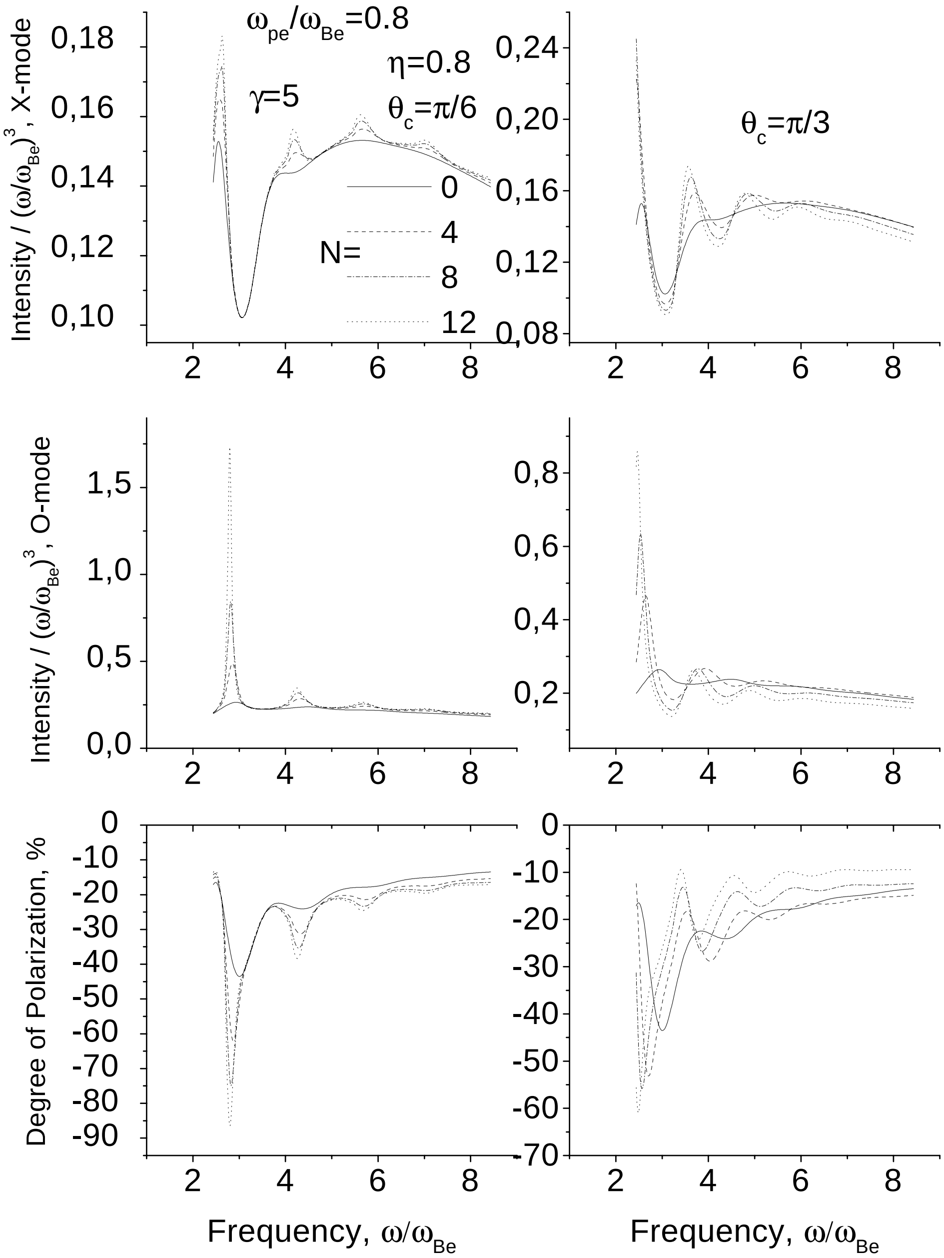

FIG. 5.—Effect of angular gradient for the electron pitch-angle distribution of the loss-cone (sin-N) type. The spectral peaks become more prominent as N increases.

ECM emission in relatively tenuous plasma if the respective absorption coefficient is negative (wave amplification instead of absorption). However, there are cases in which the pitch-angle anisotropy reduces the absorption coefficient strongly while keeping it positive. An example of this situation is shown in Figure 4 (*middle left*). The emission of O-mode displays a prominent strong narrow peak at $\omega/\omega_{\rm Be} \approx 2.2$–2.3. The peak value here exceeds the mean level of the intensity by 2 orders of magnitude (the respective degree of polarization is close to 100%; Fig. 4, *left bottom*), and the bandwidth of the peak is about a few percent. These properties (high intensity, strong polarization, and narrow bandwidth) are similar to those of ECM emission. However, ECM peaks have a rather short lifetime because of quasi-linear saturation of the emission (Fleishman & Arzner 2000). We should emphasize that the narrow peaks in Figure 4 are provided entirely by the reduction of the self-absorption due to the anisotropy effect (æ is still positive), so no wave amplification occurs. Hence, the quasi-linear saturation does not happen, and the peaks can have much longer lifetime than the ECM bursts.

The enhancement of the spectral peaks is provided by a negative contribution of an angular derivative into the absorption coefficient (6). Accordingly, the stronger the gradient of the pitch-angle distribution around the loss cone, the higher the peak in the radiation spectrum. Figure 5 illustrate this property. Various curves in the figure correspond to different values of N: larger values of N describe steeper decreases of the angular distribution function near the loss-cone angle. Evidently, the main peaks (around $\omega/\omega_{\rm Be} = 2.8$

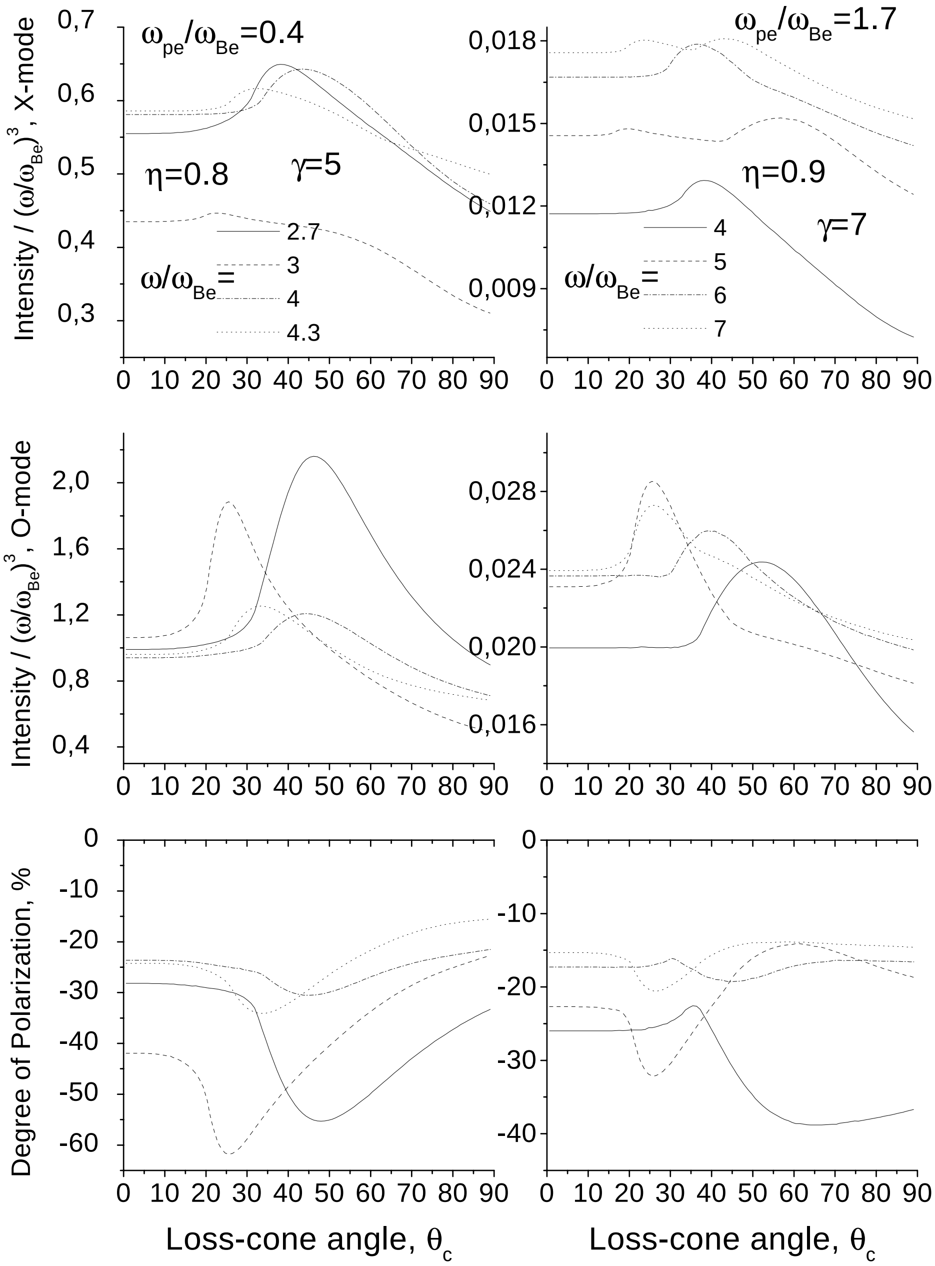

FIG. 6.—Dependence on the loss-cone width. Note that the intensity at each frequency reaches its peak for different θ_c values. The favorable θ_c varies typically between 30° and 60°.

[*left column*] and $\omega/\omega_{Be} = 2.5$ [*right column*]) become stronger for larger values of N. Weaker peaks at higher frequencies increase with N as well.

Dependence on the loss-cone angle.—Let us proceed now to the dependences of the results on the parameters of the fast electron distribution. Figure 6 displays the dependences of the radiation intensities and polarization at a few single frequencies on the loss-cone angle θ_c for $N = 6$. The frequencies are selected to match individual spectral maxima or minima in Figures 1 and 2. Typically, both O and X intensities grow, then reach a peak value, and finally decrease below the initial value with θ_c increasing (the isotropic case corresponds to $\theta_c = 0$). The peak value (at each frequency) can exceed the respective minimum by the factor 3 or so. The loss-cone angle most favorable for producing the peak varies typically between 30° and 60° for different frequencies.

The degree of polarization varies within broad interval (15%–60%) as loss-cone angle changes. The variations (of both radiation intensity and degree of polarization) become more prominent for steeper sin-N function (larger N).

Dependence on the spectral index.—Figure 7 presents the dependences of intensity and polarization spectra on the power-law index of electron momentum distribution, γ. Since the idea how the spectra depend on γ can be taken from Figures 1–3, plotted for $\gamma = 5,\ 7,$ and 9, we consider here the emission at a single frequency. The figure is plotted for various steepnesses N of the loss-cone function. Generally, the radiation intensity decreases for softer electron spectra. For the optically thick regime this can be tentatively

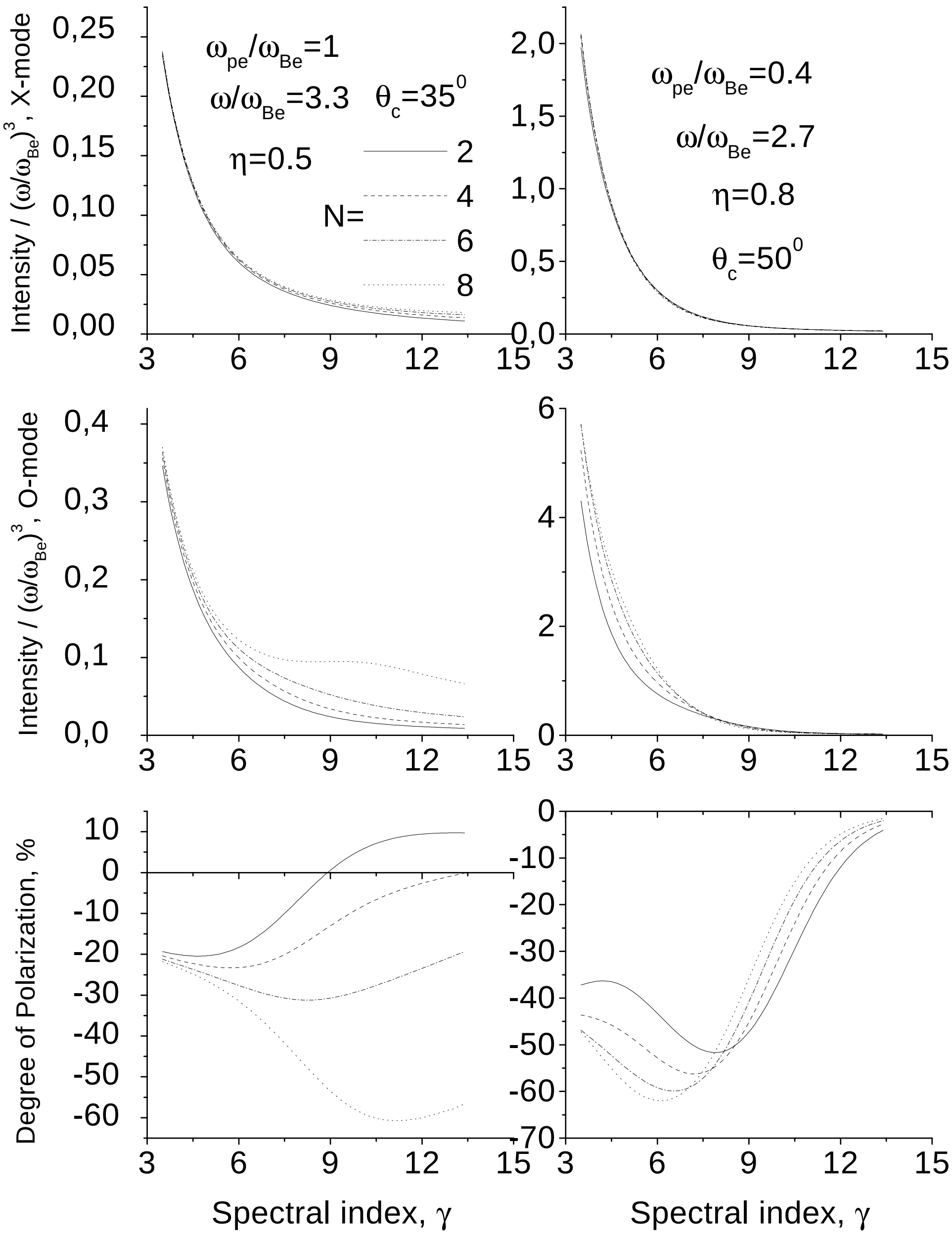

FIG. 7.—Effect of the electron spectral index. Note that the degree of polarization varies in a very wide range.

interpreted as a result of the respective decrease of an " effective temperature " of radiating electrons for softer spectra. While the effect of anisotropy is evident for radiation intensity, it is more prominent for the degree of polarization: it can either increase or decrease with γ for different values of N. The degree of polarization varies within a remarkably broad interval from -60% to $+10\%$.

Dependence on the view angle ϑ.—At some frequencies the effect of anisotropy is minor, and the resulting radiation deviates from the isotropic case only at a small range of ϑ. At other frequencies, however, the effect of anisotropy is clearly visible for a wide range of ϑ. Figure 8 shows that the anisotropic momentum distribution in a form of the loss-cone type results in lowered emission for the view angles $\vartheta < 45°–55°$ and enhanced emission for $50° < \vartheta < 70°$. At larger ϑ the effect of anisotropy becomes weak.

Effect of pitch-angle distribution shape.—To study the dependence of the results on the shape of the pitch-angle distribution, we performed calculations for a more general type of angular distribution (12) that can model a loss cone (for $\mu_1 = 0$), a beam with angular width μ_0 (for $\mu_1 = 1$), or a " hollow-beam " (for $0 < \mu_1 < 1$).

Figure 9 (*left*) displays the radiation for various μ_1 with the other parameters as in Figure 4 (*left*). While the shapes of the curves in these two figures are generally similar to each other, there are still important differences. First, the peaks are shifting as anisotropy changes. Second, relatively broad regions of positive polarization appear; the polarization can change the sense up to five times as frequency changes. Finally, the polarization is sensitive to the particle beaming: the (negative) degree of polarization enhances systematically in value as μ_1 increases from 0 to 1.

Furthermore, the main peak at $\omega/\omega_{\rm Be} \approx 2.3$ in Figure 9 (*middle left*), appears to be weaker than the respective peak in Figure 4. This indicates that the reduction of the absorption coefficient by Gaussian angular distribution is not as

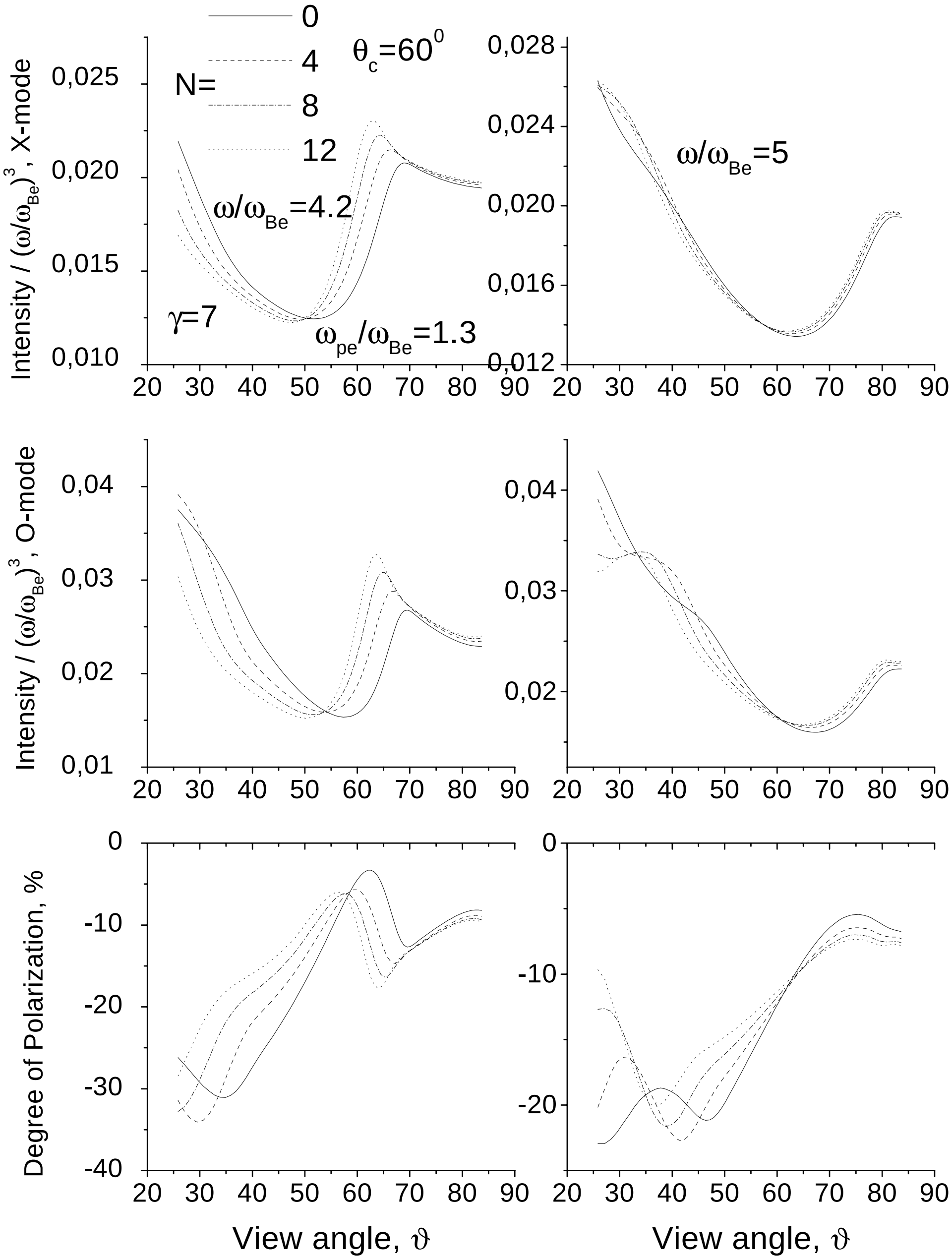

FIG. 8.—Dependence on the view angle ϑ for sin-N pitch-angle distribution for various N

efficient as the reduction by sin-N angular distribution. We should note that sin-N angular distribution is more favorable than Gaussian distribution for producing ECM emission (Fleishman & Melnikov 1998) for the very same reason.

The effect of Gaussian pitch-angle anisotropy is visible for denser plasma as well (Fig. 9, *right column*). Particularly, positions of peaks changes with μ_1.

4. DISCUSSION

The calculations performed in this study show the effect of pitch-angle anisotropy on optically thick gyrosynchrotron radiation. It is found that the pitch-angle anisotropy significantly affects both radiation intensity and degree of polarization. The mean level of the radiation intensity, especially in the quasi-parallel directions of the radiation, changes with the degree of anisotropy of electron momentum distribution. Moreover, the harmonic structure of the low-frequency radiation becomes more prominent for anisotropic distributions than it appears for the isotropic case. Very strong and narrow (~a few percent) spectral peaks arise under favorable conditions (e.g., Figs. 4 and Fig. 5, *middle left panels*) when the distribution of fast electrons is close to, but still below, the threshold for ECM instability.

The mean value of the degree of polarization can change considerably as a result of pitch-angle anisotropy (Figs. 1–5 and Fig. 9) and can even change the sense of polarization (Fig. 9). Obviously, the strong spectral peaks in the intensity spectrum display a very high degree of polarization depending on frequency.

We emphasize that these properties are entirely due to the functional behavior of the electron momentum distribution

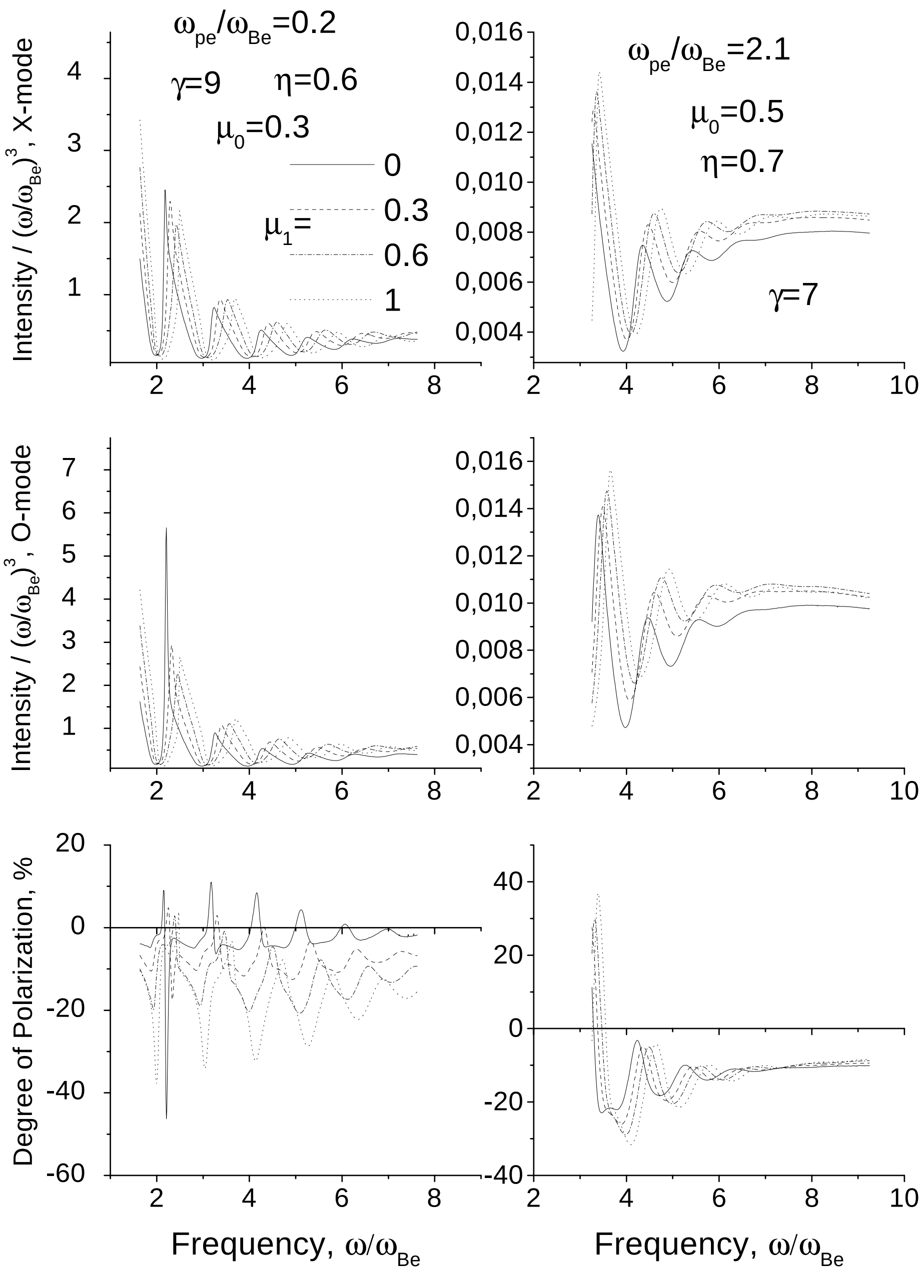

FIG. 9.—Effect of angular distribution shape. Compare the emission produced by Gaussian distribution (*left column*) with that produced by sin-N distribution (Fig. 4). The right column displays the effect of density: spectral variations (peaks) become weaker as the density increases.

and its derivatives over p and μ, differing from those of an isotropic distribution. Since both values j and æ are proportional to the number of electrons, the optically thick intensity is independent on the number of electrons.

Let us discuss briefly possible applications of the results to the solar microwave bursts. As has been discussed earlier, the pitch-angle anisotropy of fast electrons in flares is likely to occur. However, actual inhomogeneity of the emission source (including magnetic field nonuniformity) affects the resulting radiation. It should be noted that the change of the mean level of the radiation intensity and degree of polarization due to pitch-angle anisotropy must survive after averaging over the source inhomogeneity and, thus, should be observable even for observations with low spatial resolution. However, the spectral peaks could be smoothed out by the averaging; hence, spatially resolved observations are required to observe them.

The spectral peaks could have been observed without spatial resolution only for sources with a pretty constant magnetic field. Kundu et al. (2001) derive a constancy of magnetic field for a particular solar microwave burst. If their interpretation is correct, the low-frequency (optically thick) component of the burst should display spectral peaks (related to either isotropic or anisotropic distribution of fast electrons). Conversely, observations of the low-frequency component could be used to test the idea of constant magnetic field.

It is important that the discovered strong narrow peaks are different from ECM peaks because no wave amplification occurs. Hence, the effect of emitted waves on pitch-angle distribution is negligible, so the considered spectral peaks can have a much longer lifetime than the respective ECM peaks. Some low-frequency (1–3 GHz) peaks with moderate duration have occasionally been observed with the OVSA (J. Lee 2001, private communication).

Obviously, the effect of pitch-angle anisotropy appears to be even much more essential for the new planned generation of the solar-dedicated multifrequency radio instruments such as FASR (Bastian et al. 1998) and the upgraded SSRT (Smolkov et al. 2000), which are expected to provide both high spatial and spectral resolution.

Finally, we would like to stress that the anisotropy effect is also (or even more) important for the optically thin regime and for the region of gyrosynchrotron spectral maximum, which is studied in a forthcoming paper.

The work was supported by the Russian Foundation for Basic Research grants 00-02-16356, 01-02-16586, and 02-02-39005, the Russian Federal Program "Astronomy," NFSC project 19833050, the "973" program with grant G2000078403, and NSF grant AST 99-87366 to the New Jersey Institute of Technology. V. M. is grateful to the National Astronomical Observatory of Japan for support of his visit to NRO.

APPENDIX

The polarization vector $\boldsymbol{e}_{\sigma,\boldsymbol{k}}$ of σ-mode wave ($\sigma = 1$ for O-mode and $\sigma = -1$ for X-mode) in the reference frame with z-axis along the magnetic field $\boldsymbol{B}$ and the $\boldsymbol{k}$-vector in the $(y,\ z)$ plane is

$$\boldsymbol{e}_{\sigma,\boldsymbol{k}} = \frac{(1,\ i\alpha_\sigma,\ i\beta_\sigma)}{(1+\alpha_\sigma^2+\beta_\sigma^2)^{1/2}}\ , \tag{A1}$$

where

$$\alpha_\sigma = K_\sigma\cos\theta - \Gamma_\sigma\sin\theta\ , \qquad \beta_\sigma = K_\sigma\sin\theta + \Gamma_\sigma\cos\theta\ , \tag{A2}$$

$$K_\sigma = \frac{2\sqrt{u}(1-v)\cos\theta}{u\sin^2\theta - \sigma\left[u^2\sin^4\theta + 4u(1-v)^2\cos^2\theta\right]^{1/2}}\ ,$$
$$K_X K_O = -1\ , \tag{A3}$$

$$\Gamma_\sigma = -\frac{v\sqrt{u}\sin\theta + uvK_\sigma\cos\theta\sin\theta}{1-u-v(1-u\cos^2\theta)}\ , \tag{A4}$$

$$v = \omega_{pe}^2/\omega^2\ , \qquad u = \omega_{\mathrm{Be}}^2/\omega^2\ . \tag{A5}$$

The refractive indices have the form

$$n_\sigma^2 = 1 - \frac{2v(1-v)}{2(1-v) - u\sin^2\theta + \sigma\left[u^2\sin^4\theta + 4u(1-v)^2\cos^2\theta\right]^{1/2}}\ . \tag{A6}$$

REFERENCES

Alfvén, N., & Herlofson, N. 1950, Phys. Rev., 78, 616
Aschwanden, M. J., & Benz, A. O. 1988, ApJ, 332, 447
Aschwanden, M. J., Benz, A. O., Schwartz, R. A., Lin, R. P., Pelling, R. M., & Stehling, W. 1990, Sol. Phys., 130, 39
Bastian, T. S., Benz, A. O., & Gary, D. E. 1998, ARA&A, 36, 131
Bastian, T. S., Bookbinder, J., Dulk, G. A., & Davis, M. 1990, ApJ, 353, 265
Bastian, T. S., Gary, D. E., White, S. M., & Hurford, G. J. 1998, Proc. SPIE, 3357, 609
Benka, S. G., & Holman, G. D. 1992, ApJ, 391, 854
Dulk, G. A., & Marsh, K. A. 1982, ApJ, 259, 350
Eidman, V. Ya. 1958, Soviet Phys.–JETP, 7, 91
———. 1959, Soviet Phys.–JETP, 9, 947
Fleishman, G. D. 1994, Sol. Phys., 153, 367
Fleishman, G. D., & Arzner, K. 2000, A&A, 358, 776
Fleishman, G. D., & Melnikov, V. F. 1998, Phys. Uspekhi, 41, 1157
———. 2003, ApJ, in press
Fleishman, G. D., & Yastrebov, S. G. 1994, Sol. Phys., 153, 389
Gary, D. E., & Hurford, G. J. 1999, in Solar Physics with Radio Observations, ed. T. S. Bastian, N. Gopalswamy, & K. Shibasaki (NRO Rep. 479; Minamisaku: Nobeyama Radio Obs.), 429
Getmantsev, G. G. 1952, Dokl. Akad. Nauk SSSR, 83, 557
Ginzburg, V. L. 1951, Dokl. Akad. Nauk SSSR, 76, 377
Ginzburg, V. L., & Syrovatsky, S. I. 1964, The Origin of Cosmic Rays (New York: Macmillan)
Hewitt, R. G., Melrose, D. B., & Rönnmark, K. G. 1982, Australian J. Phys. 35, 447
Huang, G.-L. 1987, Sol. Phys., 114, 363
Kiepenheuer, K. O. 1950, Phys. Rev., 79, 738
Klein, K.-L. 1987, A&A, 183, 341
Kundu, M. R., Nindos, A., White, S. M., & Grechnev, V. V. 2001, ApJ, 557, 880
Ledenev, V. G. 1998, Sol. Phys., 179, 405
Lee, J., & Gary, D. E. 2000, ApJ, 543, 457
Li, H. W. 1986, Sol. Phys., 104, 131
McTiernan, J. M., & Petrosian, V. 1991, ApJ, 379, 381
Melnikov, V. F. 1994, Radiophys. Quantum Electron., 37, 557
Melnikov, V. F., & Magun, A. 1998, Sol. Phys., 178, 153
Melnikov, V. F., Shibasaki, K., & Reznikova, V. E. 2002, ApJ, 580, L185
Melnikov, V. F., Shibasaki, K., Yokoyama, T., Nakajima, H., & Reznikova, V. E. 2001, Abstracts of the CESRA Workshop, 2001 July 2–6, Munich, Germany
Melrose, D. B., Rönnmark, K. G., & Hewitt, R. G. 1982, J. Geophys. Res. 87, 5140
Nakajima, H., et al. 1994, Proc. IEEE, 82, 705
Petrosian, V. 1982, ApJ, 255, L85

Pryadko, J. M., & Petrosian, V. 1999, ApJ, 515, 873
Ramaty, R. 1969, ApJ, 158, 753
Ramaty, R., Schwarz, R. A., Enome, S., & Nakajima, H. 1994, ApJ, 436, 941
Razin, V. A. 1960, Radiofiz., 3, 584
Robinson, P. A. 1985, ApJ, 298, 161
Sharma, R. R., & Vlahos, L. 1984, ApJ, 280, 405
Smolkov, G. J., Zandanov, V. G., & Altyntsev, A. T. 2000, Proc. SPIE, 4015, 197
Takakura, T. 1972, Sol. Phys., 26, 151
Vlasov, V. G., Kuznetsov, A. A., & Altyntsev, A. T. 2002, A&A, 382, 1061
Wu, C. S., & Lee, L. C. 1979, ApJ, 230, 621
Zhou, A. H., & Huang, G.-L. 2001, Chinese J. Astron. Astrophys., 1, 365